## Anatomical Region Definitions

| Region # | Region Name | Region # | Region Name | Region # | Region Name |
|---|---|---|---|---|---|
| 1 | Insular_ctx_L | 41 | Inf_Temp_G_post_R | 81 | Cerebellum |
| 2 | Ant_Dorsolateral_Frontal_ctx_L | 42 | Postcentral_G_R | 82 | Brain Stem |
| 3 | Precentral_G_L | 43 | Parietal_Lobule_R | 83 | Anterior_Medial_Frontal_ctx_R |
| 4 | Anterior_Temp_Pole_L | 44 | Supramarginal_G_R | 84 | Poster_Medial_Frontal_ctx_R |
| 5 | Sup_Temp_G_ant_L | 45 | Angular_G_R | 85 | Anterior_Medial_Frontal_ctx_L |
| 6 | Sup_Temp_G_post_L | 46 | Occipital_Pole_R | 86 | Poster_Medial_Frontal_ctx_L |
| 7 | Middle_Temp_G_ant_L | 47 | Calcarine_ctx_R | 87 | Post_Dorsolateral_Frontal_ctx_L |
| 8 | Middle_Temp_G_post_L | 48 | Medial_Orbital_ctx_R | 88 | Post_Dorsolateral_Frontal_ctx_R |
| 9 | Inf_Temp_G_ant_L | 49 | SMA_R | 89 | Putamen_R |
| 10 | Inf_Temp_G_post_L | 50 | Precuneous_ctx_R | 90 | Putamen_L |
| 11 | Postcentral_G_L | 51 | Cuneus_R | | |
| 12 | Parietal_Lobule_L | 52 | Lat_Orbital_ctx_R | | |
| 13 | Supramarginal_G_L | 53 | Parahip_Ambiens_G_ant_R | | |
| 14 | Angular_G_L | 54 | Parahip_Subiculum_G_post_R | | |
| 15 | Occipital_Pole_L | 55 | Lingual_G_R | | |
| 16 | Calcarine_ctx_L | 56 | Temp_Fusiform_ctx_ant_R | | |
| 17 | Medial_Orbital_ctx_L | 57 | Temp_Fusiform_ctx_post_R | | |
| 18 | SMA_L | 58 | Temp_Occip_Fusiform_ctx_R | | |
| 19 | Precuneous_ctx_L | 59 | Occipital_Fusiform_G_R | | |
| 20 | Cuneus_L | 60 | Frontal_Operculum_ctx_R | | |
| 21 | Lat_Orbital_ctx_L | 61 | Central_Operculum_ctx_R | | |
| 22 | Parahip_Ambiens_G_ant_L | 62 | Parietal_Operculum_ctx_R | | |
| 23 | Parahip_Subiculum_G_post_L | 63 | Ventral_Cing_Subcallosal_G | | |
| 24 | Lingual_G_L | 64 | Anterior_Cingulate_G | | |
| 25 | Temp_Fusiform_ctx_ant_L | 65 | Posterior_Cingulate_G | | |
| 26 | Temp_Fusiform_ctx_post_L | 66 | Dorsal_Anterior_Cingulate | | |
| 27 | Temp_Occip_Fusiform_ctx_L | 67 | Cerebral_White_Matter_L | | |
| 28 | Occipital_Fusiform_G_L | 68 | Caudate_L | | |
| 29 | Frontal_Operculum_ctx_L | 69 | Globus_Pallidus_L | | |
| 30 | Central_Operculum_ctx_L | 70 | Hippocampus_L | | |
| 31 | Parietal_Operculum_ctx_L | 71 | Amygdala_L | | |
| 32 | Insular_ctx_R | 72 | Accumbens_L | | |
| 33 | Ant_Dorsolateral_Frontal_ctx_R | 73 | Cerebral_White_Matter_R | | |
| 34 | Precentral_G_R | 74 | Caudate_R | | |
| 35 | Anterior_Temp_Pole_R | 75 | Globus_Pallidus_R | | |
| 36 | Sup_Temp_G_ant_R | 76 | Hippocampus_R | | |
| 37 | Sup_Temp_G_post_R | 77 | Globus_Pallidus_R | | |
| 38 | Middle_Temp_G_ant_R | 78 | Hippocampus_R | | |
| 39 | Middle_Temp_G_post_R | 79 | Thalamus_L | | |
| 40 | Inf_Temp_G_ant_R | 80 | Thalamus_R | | |

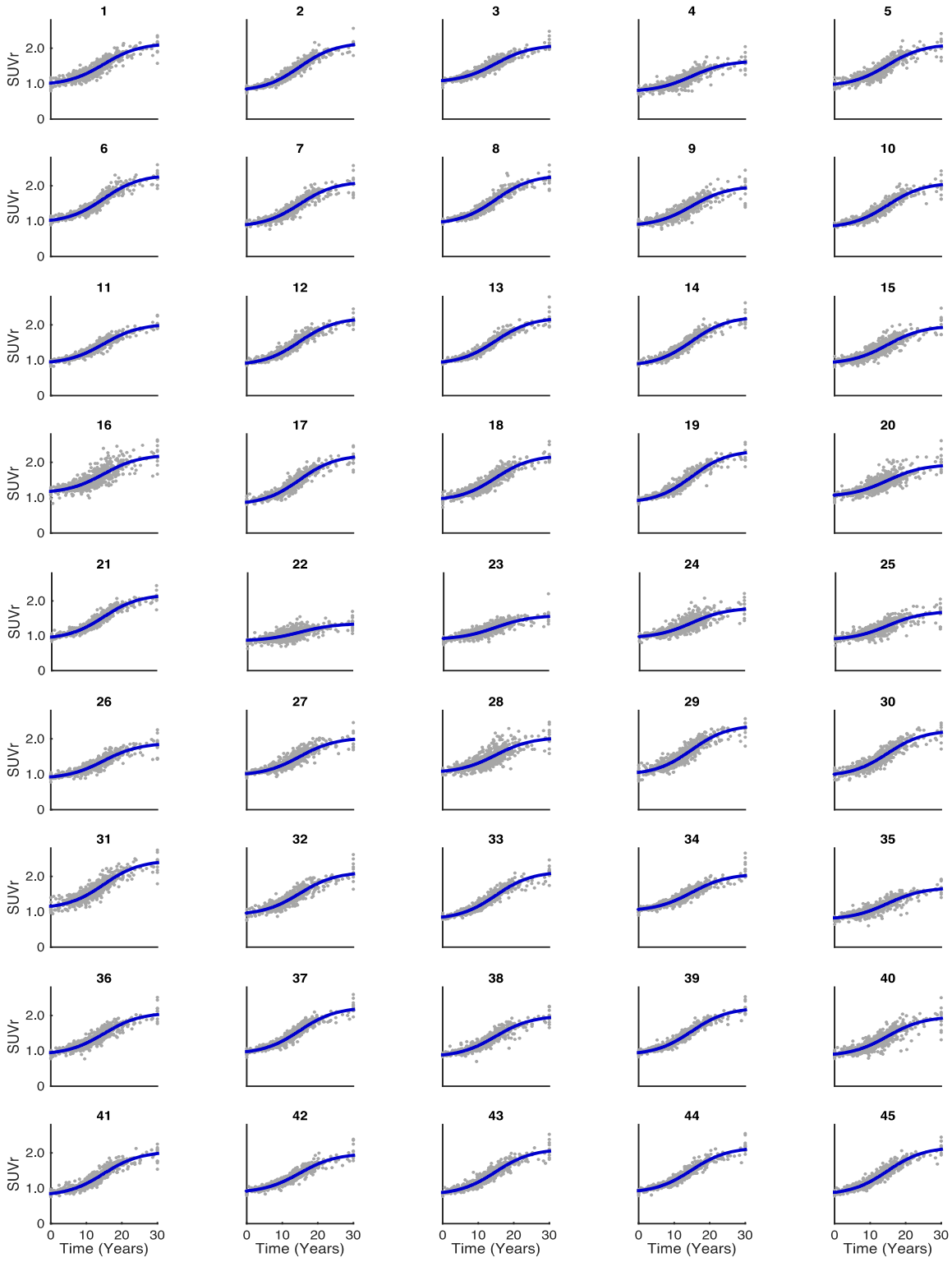


**Supplemental Figure 1:** Fit of the most parsimonious logistic growth model to the chronological $^{18}$F-AV45 Aβ PET data with a single uninhibited exponential growth rate (r = 0.20 yrs$^{-1}$) and a single time of half maximal Aβ concentration ($T_{50}$ = 14.9 yrs) for all brain regions in the CIC neuroanatomical atlas (Regions 1-45).

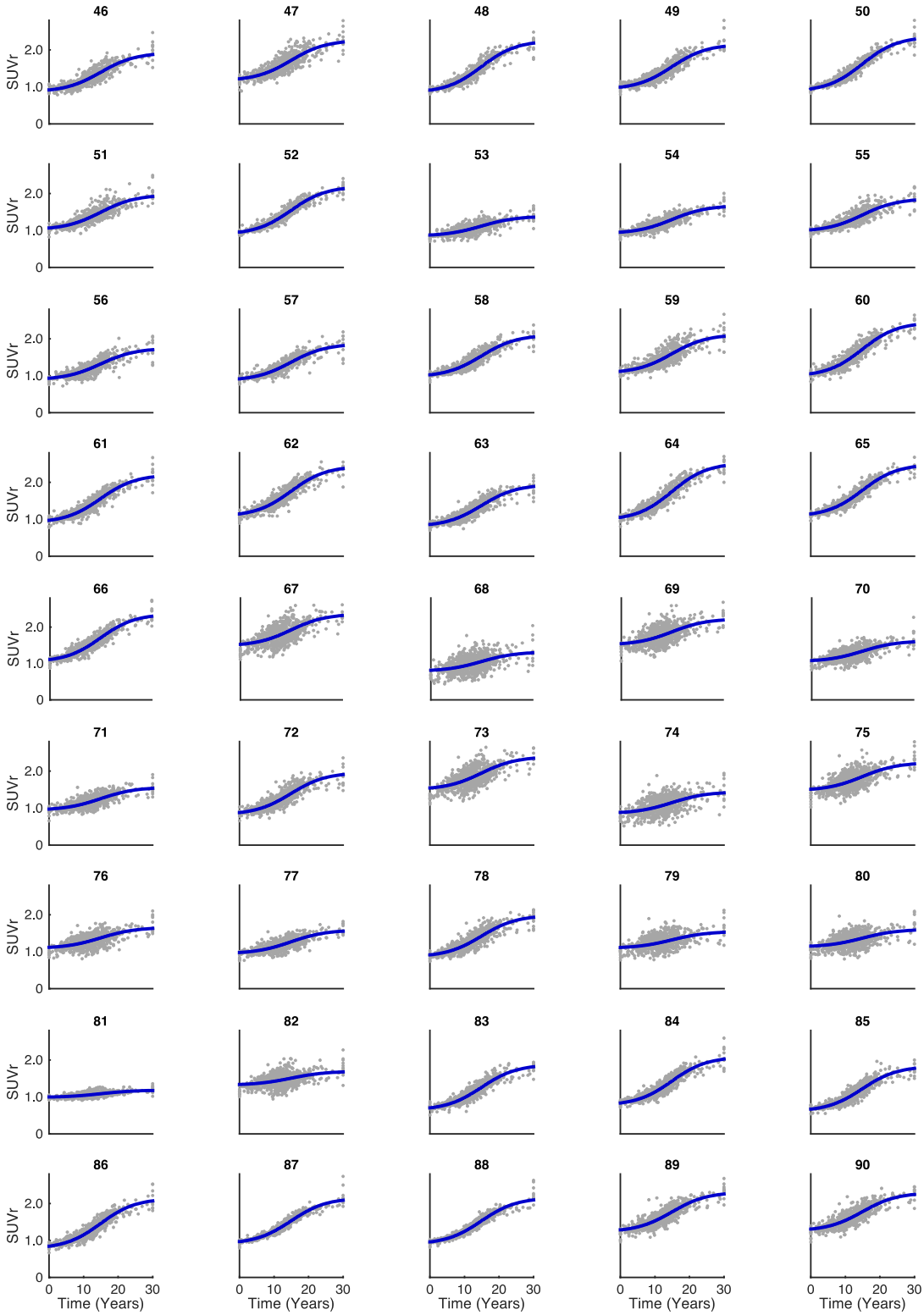


**Supplemental Figure 2:** Fit of the most parsimonious logistic growth model to the chronological $^{18}$F-AV45 Aβ PET data with a single uninhibited exponential growth rate (r = 0.20 yrs$^{-1}$) and a single time of half maximal Aβ concentration ($T_{50}$ = 14.9 yrs) for all brain regions in the CIC neuroanatomical atlas (Regions 45-90).

**Parametric Imaging**

Model 11 was linearized for fast and robust fitting at the voxel-level using fixed values for r and $T_{50}$ obtained from the regional analysis. The original model equation

$$SUVr(t) = NS + \frac{K}{1+e^{-r(t-T_{50})}}.$$

is transformed into a linear equation of the form,

$$b = A\,x$$

where

$$A = \begin{bmatrix} 1 & \frac{1}{1+e^{-r(t_1-T_{50})}} \\ \vdots & \vdots \\ 1 & \frac{1}{1+e^{-r(t_{769}-T_{50})}} \end{bmatrix} \begin{bmatrix} NS_{vox} \\ K_{vox} \end{bmatrix},$$

$$x = \begin{bmatrix} NS_{vox} \\ K_{vox} \end{bmatrix},$$

$$b = SUVr(t)$$

$NS_{vox}$ and $K_{vox}$ are the non-specific binding and the carrying capacity for the voxel respectively. These parameters were then estimated by solving the linear equation in MATLAB using

$$x = A\backslash b\ . \qquad (11)$$

**Calculation with different ROI sets**

We have run the analysis process on 2 additional sets of ROIs. A set of 9 ROIs which are much larger regions and cover the whole brain along with a parcellation that is restricted to cortical region sand includes 76 regions (this corresponds to the removal of the sub-cortical regions from the previous set of 90 ROIs where there is lower accumulation).

For both these additional analyses the same model (Model 11) is identified as the most parsimonious description of the data. This provides strong evidence that this result is not dependent on the choice of regions or due to lack of statistical power in measuring changes in $T_{50}$.

**Supplemental Table 1:** Analogous table to Table 2 using 9 large ROIs covering the whole cerebrum. As with the analysis using a 90 region atlas, Model 11 is selected as the optimum model.

| Model | K SUVr | r $yrs^{-1}$ | $T_{50}$ yrs | NS | Parameters | SSQ | $\Delta BIC_i$ ($BIC_i$ - $BIC_{min}$) |
|---|---|---|---|---|---|---|---|
| Model 1 | Global | Global | Global | Global | 4 | 434.4 | 12722.3 |
| Model 2 | Global | Local | Global | Global | 12 | 227.7 | 8322.39 |
| Model 3 | Local | Global | Global | Global | 12 | 126.9 | 4275.26 |
| Model 4 | Global | Global | Local | Global | 12 | 106.2 | 3042.9 |
| Model 5 | Global | Global | Global | Local | 12 | 94.15 | 2209.86 |
| Model 6 | Local | Local | Global | Global | 20 | 103.5 | 2938.7 |
| Model 7 | Local | Global | Local | Global | 20 | 90.9 | 2037.42 |
| Model 8 | Global | Local | Local | Global | 20 | 86.13 | 1663.84 |
| Model 9 | Global | Global | Local | Local | 20 | 74.93 | 700.218 |
| Model 9 | Global | Local | Global | Local | 20 | 77.4 | 924.902 |
| Model 11 | Local | Global | Global | Local | 20 | 67.72 | 0 |
| Model 12 | Local | Local | Local | Global | 28 | 84.44 | 1597.98 |
| Model 13 | Local | Global | Local | Local | 28 | 67.64 | 62.0933 |
| Model 14 | Global | Local | Local | Local | 28 | 67.62 | 60.4626 |
| Model 15 | Local | Local | Global | Local | 28 | 67.05 | 1.398 |
| Model 16 | Local | Local | Local | Local | 36 | 67.01 | 68.2141 |

**Supplemental Table 2:** Analogous table to Table 2 using 76 cortical ROIs. Model 11 is again selected as the optimum model.

| Model | K SUVr | r $yrs^{-1}$ | $T_{50}$ yrs | NS | Parameters | SSQ | $\Delta BIC_i$ ($BIC_i$ - $BIC_{min}$) |
|---|---|---|---|---|---|---|---|
| Model 1 | Global | Global | Global | Global | 4 | 1257 | 74781.8 |
| Model 2 | Global | Local | Global | Global | 79 | 895.3 | 55777.2 |
| Model 3 | Local | Global | Global | Global | 79 | 484.3 | 19862.4 |
| Model 4 | Global | Global | Local | Global | 79 | 456.4 | 16390.7 |
| Model 5 | Global | Global | Global | Local | 79 | 400.4 | 8738.36 |
| Model 6 | Local | Local | Global | Global | 154 | 392 | 8334.23 |
| Model 7 | Local | Global | Local | Global | 154 | 394.3 | 8673.35 |
| Model 8 | Global | Local | Local | Global | 154 | 403.8 | 10063.6 |
| Model 9 | Global | Global | Local | Local | 154 | 381.8 | 6792.16 |
| Model 10 | Global | Local | Global | Local | 154 | 347.4 | 1268.12 |
| Model 11 | Local | Global | Global | Local | 154 | 339.9 | 0 |
| Model 12 | Local | Local | Local | Global | 229 | 371.3 | 5980.34 |
| Model 13 | Local | Global | Local | Local | 229 | 339.6 | 758.079 |
| Model 14 | Global | Local | Local | Local | 229 | 339.7 | 790.638 |
| Model 15 | Local | Local | Global | Local | 229 | 336.7 | 272.73 |
| Model 16 | Local | Local | Local | Local | 304 | 336.1 | 976.546 |